

RESEARCH ARTICLE

Cxcl12a induces *snail1b* expression to initiate collective migration and sequential Fgf-dependent neuromast formation in the zebrafish posterior lateral line primordium

Uma M. Neelathi, Damian Dalle Nogare and Ajay B. Chitnis*

ABSTRACT

The zebrafish posterior lateral line primordium migrates along a path defined by the chemokine Cxcl12a, periodically depositing neuromasts, to pioneer formation of the zebrafish posterior lateral line system. *snail1b*, known for its role in promoting cell migration, is expressed in leading cells of the primordium in response to Cxcl12a, whereas its expression in trailing cells is inhibited by Fgf signaling. *snail1b* knockdown delays initiation of primordium migration. This delay is associated with aberrant expansion of *epithelial cell adhesion molecule* (*epcam*) and reduction of *cadherin 2* expression in the leading part of the primordium. Co-injection of *snail1b* morpholino with *snail1b* mRNA prevents the initial delay in migration and restores normal expression of *epcam* and *cadherin 2*. The delay in initiating primordium migration in *snail1b* morphants is accompanied by a delay in sequential formation of trailing Fgf signaling centers and associated protoneuromasts. This delay is not specifically associated with knockdown of *snail1b* but also with other manipulations that delay migration of the primordium. These observations reveal an unexpected link between the initiation of collective migration and sequential formation of protoneuromasts in the primordium.

KEY WORDS: Cxcl12a, Cell adhesion molecule, Collective migration, Lateral line primordium, Snail1b, Zebrafish

INTRODUCTION

Interactions between cells determine morphogenesis, cell fate and cell behavior in developing organs. The simplicity and accessibility of the zebrafish posterior lateral line (pLL) system and our ability to manipulate and monitor its development in live embryos has led to its establishment as an extremely effective model system for studying self-organization of developing organ systems. The lateral line is a sensory system that allows fish to sense the pattern of water flow over the surface of their bodies (Coombs and Montgomery, 1999). It consists of sensory organs called neuromasts that are distributed in a stereotyped pattern over the body surface. Each neuromast has a cluster of sensory hair cells at its center. They are innervated by neurons of the lateral line ganglia, which carry sensory information from neuromasts back to the brain (Ghyssen and Dambly-Chaudière, 2007).

Formation of the pLL system in zebrafish is pioneered by the pLL primordium, a group of about 140 cells that separates from the pLL placode, leaving behind cells that form the sensory neurons of the pLL ganglion (Kimmel et al., 1995). Whereas leading cells in the pLL primordium have a quasi-mesenchymal morphology, trailing cells are more epithelial; they have distinct apical-basal polarity and they reorganize to form nascent neuromasts (protoneuromasts) sequentially (Lecaudey et al., 2008; Nechiporuk and Raible, 2008). The primordium begins migration toward the tip of the tail at about 22 h post-fertilization (hpf). Cells incorporated into protoneuromasts in the migrating primordium are deposited as neuromasts, whereas cells that were not are deposited between neuromasts as inter-neuromast cells. Eventually, the primordium ends its migration about 24 h later after depositing five or six neuromasts and by resolving into two or three terminal neuromasts (Sarrazin et al., 2010).

Establishment of polarized Wnt and Fgf signaling systems coordinates morphogenesis and migration of the primordium. Wnt signaling dominates at the leading end and promotes its own activity (Aman and Piotrowski, 2008; Jiang et al., 2014). At the same time, activation of the Wnt/ β -catenin signaling pathway drives expression of *fgf3* and *fgf10*. However, leading cells, which produce Fgf, do not respond to these signals because Wnt activity simultaneously promotes expression of factors that inhibit activation of Fgf receptors (Aman and Piotrowski, 2008; Matsuda et al., 2013). Instead, the Fgfs activate Fgf signaling at the trailing end of the primordium, where Wnt signaling is weakest. There, Fgf signaling determines expression of the diffusible Wnt antagonist Dkk1b, which counteracts Wnt signaling to help establish stable Fgf-responsive signaling centers (Aman and Piotrowski, 2008). Once established, activation of the Fgf signaling pathway in trailing cells coordinates morphogenesis of protoneuromasts by simultaneously promoting the reorganization of cells into epithelial rosettes and by initiating expression of factors that help specify a hair cell progenitor at the center of each forming neuromast (Itoh and Chitnis, 2001; Lecaudey et al., 2008; Matsuda and Chitnis, 2010; Nechiporuk and Raible, 2008). Over time, the initially broad Wnt active domain shrinks closer to the leading edge and additional Fgf signaling centers form sequentially in its wake, each associated with formation of additional protoneuromasts (Dalle Nogare and Chitnis, 2017).

Polarized Wnt-Fgf signaling systems in the pLL primordium also coordinate collective migration of the primordium along the horizontal myoseptum on a path defined by the chemokine Cxcl12a (previously known as Sdf1a) (Sapede et al., 2005). Directed migration of the primordium in a caudal direction is determined by the polarized expression of two chemokine receptors, Cxcr4b and Cxcr7b (Acker3b – Zebrafish Information Network) (Dambly-Chaudière et al., 2007; Haas and Gilmour, 2006; Valentin

Section on Neural Developmental Dynamics, Division of Developmental Biology, Eunice Kennedy Shriver National Institute of Child Health and Human Development, National Institutes of Health, Bethesda, MD 20892, USA.

*Author for correspondence (chitnisa@mail.nih.gov)

© A.B.C., 0000-0002-6423-6624

Received 12 December 2017; Accepted 13 June 2018

et al., 2007). Cells in the leading two thirds of the primordium express *cxc7b*, which encodes a chemokine receptor that allows cells to interact with Cxcl12a and to respond via G protein-coupled signaling pathways with migratory behavior. The absence of Wnt signaling allows expression of *cxc7b* in the trailing part of the primordium (Aman and Piotrowski, 2008). Cxcr7b interacts with Cxcl12a but its distinctive intracellular domain cannot engage the G protein-coupled system to determine migratory behavior (Balabanian et al., 2005; Graham, 2009). As a result, the migratory response of leading cells, coupled with unresponsive trailing cells, determines polarized response to Cxcl12a in the path of the primordium. In addition, Cxcl12a binds Cxcr7b with greater affinity than it does with Cxcr4b (Balabanian et al., 2005). Once bound, the complex is internalized and Cxcr7b-expressing cells degrade Cxcl12a. This creates a local gradient of Cxcl12a, which contributes to the robust polarized migratory response of leading primordium cells to Cxcl12a in the path (Donà et al., 2013; Venkiteswaran et al., 2013).

Although the framework described above provides a broad description of the early self-organization of the pLL primordium, the mechanisms that link the dynamics of Wnt-Fgf signaling to systematic changes in cell morphology, organization and migratory behavior remain poorly understood. The transcription factor Snail is well known for its role in coordinating expression of factors that promote epithelial mesenchymal transition (EMT) and migratory behavior (Barrallo-Gimeno and Nieto, 2005; Lamouille et al., 2014). An initial screen to identify factors expressed in the primordium that might promote mesenchymal morphology revealed that *snail1b* (*snail1b* – Zebrafish Information Network) is expressed in leading cells of the primordium. Its expression in the leading zone suggested that Wnt-dependent *snail1b* expression might determine the relatively mesenchymal morphology and

migratory potential of leading cells. However, as this study describes, *snail1b* expression is not dependent on Wnt signaling, nor does interfering with its function, in any obvious way, prevent leading cells from acquiring a mesenchymal morphology. Instead, we discovered that *snail1b* expression is initiated by chemokines first encountered by leading primordium cells and its expression plays a crucial role in initiating collective migration of the pLL primordium. Furthermore, we found that migratory behavior of the primordium, more generally, has an essential role in initiating sequential formation of protoneuromasts and the progressive shrinking of the Wnt system.

RESULTS

snail1b is expressed in leading cells of the pLL primordium

snail1b is expressed in leading cells of the pLL primordium at 32 hpf (Fig. 1A, arrow) and in underlying cells of the horizontal myoseptum over which the primordium migrates. As a result, in some whole-mount *in situ* hybridization images of the pLL primordium, *snail1b* expression is also seen, slightly out of focus at a deeper plane, under the primordium (Fig. 1A, arrowhead; Fig. S1A-E). *snail1b* is expressed at the leading end of the pLL primordium at 20 hpf, just before onset of collective migration, and continues to be expressed during migration (Fig. S1A-E). Its expression in the pLL primordium is lost once its migration is complete at about 48 hpf (data not shown).

snail1b expression is not dependent on Wnt signaling in leading cells

Like *snail1b*, Wnt-dependent expression of *lef1* is restricted to a leading zone of the primordium at 32 hpf (Fig. 1A,B). However, in contrast to *lef1*, expression of which initially spans the entire primordium and gradually becomes restricted to a smaller leading

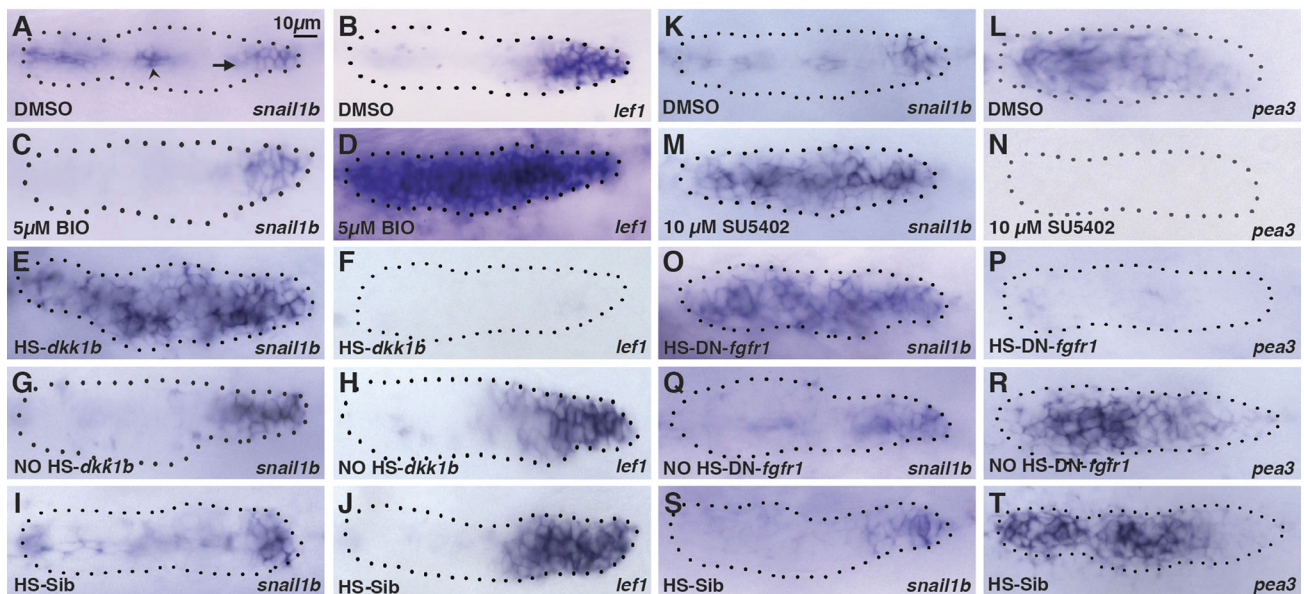


Fig. 1. Wnt-dependent Fgf signaling inhibits *snail1b* expression in the trailing domain. (A,B) Expression of *snail1b* and Wnt-dependent *lef1* in leading domain of pLL primordium in control DMSO-treated embryos at 32 hpf. Arrow and arrowhead show *snail1b* in the pLL primordium and in the underlying horizontal myoseptum cells, respectively. (C,D) *snail1b* and *lef1* expression in BIO-treated embryos. (E-J) *snail1b* and *lef1* expression following heat shock in HS:*dkk1b* embryos (E,F), without heat shock in HS:*dkk1b* embryos (G,H) and with heat shock in non-transgenic siblings (I,J). (K,L) Expression of *snail1b* and Fgf-dependent *pea3* at 32 hpf in control DMSO-treated embryos. (M,N) *snail1b* and *pea3* expression in SU5402-treated embryos. (O-T) *snail1b* and *pea3* expression following heat shock in HS:DN-*fgfr1* embryos (O,P), without heat shock in HS:DN-*fgfr1* embryos (Q,R), and with heat shock in non-transgenic siblings (S,T). Fluorescent anti-GFP staining in the *Tg(cldnb:lynGFP)* line was used to define the outline of all pLL primordia (dotted line). The primordia leading end is always to the right. *n*=20 for each of three independent experiments.

zone (Matsuda et al., 2013; Valdivia et al., 2011), *snail1b* expression is always restricted to the leading end (Fig. S1A-E). Nevertheless, we investigated whether Wnt signaling plays some role in determining *snail1b* expression in leading cells by examining embryos treated with the glycogen synthase kinase 3 inhibitor BIO, which exaggerates Wnt/ β -catenin signaling (Meijer et al., 2003). Whereas *lef1* expression expanded into the trailing domain following exposure to BIO, *snail1b* expression was indistinguishable from controls (Fig. 1C,D). This suggested that Wnt signaling does not promote expression of *snail1b*. However, when the secreted Wnt antagonist Dkk1b was expressed in response to heat shock using a HS-*dkk1b* transgenic fish line (Stoick-Cooper et al., 2007), *snail1b* expression expanded into the trailing domain, whereas it resulted in the loss of *lef1* expression in the primordium (Fig. 1E,F). No change in expression of *snail1b* and *lef1* was observed in embryos not exposed to heat shock and in heat-shocked non-transgenic controls (Fig. 1G-J). These observations show that, rather than promoting its expression, some Wnt-dependent process prevents *snail1b* expression in the trailing zone.

***snail1b* expression is inhibited by Wnt-dependent Fgf signaling in the trailing zone**

As Fgfs expressed in response to Wnt signaling determine activation of Fgf receptors in the trailing zone, we investigated whether *snail1b* expression is prevented in this region by Fgf signaling. *snail1b*, usually confined to the leading region, expanded into the trailing domain in embryos treated with the Fgf signaling inhibitor SU5402 (Mohammadi et al., 1997), whereas Fgf-dependent *pea3* (*etv4* – Zebrafish Information Network) expression was lost (Aman and Piotrowski, 2008) (Fig. 1K-N). Similarly, expression of a dominant-negative form of the Fgf receptor under control of a heat shock promoter expanded expression of *snail1b* and suppressed *pea3* expression (Fig. 1O,P) in HS-DN-*fgfr1* transgenic embryos, whereas transgenic embryos not exposed to heat shock and heat-shocked non-transgenic siblings were not affected (Fig. 1Q-T). Together, these results confirm that Fgf signaling prevents *snail1b* expression in the trailing zone.

Cxcl12a-dependent chemokine signaling determines *snail1b* expression

As Wnt signaling does not promote *snail1b* expression, we investigated whether Cxcl12a dependent-chemokine signaling

determines *snail1b* expression in leading cells. Consistent with this possibility, *snail1b* expression was reduced or lost in embryos injected with *cxcl12a* morpholino (Fig. 2A,B). Cxcr7b, expressed by trailing cells, ensures a polarized response to chemokines by preventing trailing cells from responding to Cxcl12a and knockdown of *cxcr7b* allows cells at both ends of the primordium to respond to Cxcl12a (Valentin et al., 2007). Consistent with this change, *snail1b* expression was seen at both ends of the primordium in *cxcr7b* morphants (Fig. 2C, brackets). Furthermore, heat shock-induced expression of *cxcl12a* in HS:*cxcl12a* transgenic fish transiently promoted *snail1b* expression in the entire primordium (Fig. 2D), whereas no change was seen in non-heat-shocked HS:*cxcl12a* transgenic and heat-shocked non-transgenic embryos (Fig. 2E,F). Heat shock induced broad ectopic expression of *cxcl12a*, whereas no change was seen in non-heat-shocked transgenic and heat-shocked non-transgenic controls (Fig. 2G-I).

Functional analysis of *snail1b* using morpholino oligonucleotides

Two morpholinos were used to study *snail1b* function, a translation-blocking morpholino (TB) that was validated in a previous publication (Blanco et al., 2007) and a splice-blocking morpholino (SB) that was validated by visualizing aberrantly spliced fragments induced by its injection in embryos (Fig. S2A,B). Potential p53 (Tp53 – Zebrafish Information Network)-dependent off-target effects in all morphants (Eisen and Smith, 2008; Robu et al., 2007) were minimized by the use of a relatively low dosage of morpholino (0.5 ng TB and 0.75 ng SB) and with co-injection of p53 morpholino.

pLL primordium migration and protoneuromast formation in *snail1b* morphants

In embryos injected with control morpholino provided by Gene Tools (see Materials and Methods), the primordium deposited five or six neuromasts and completed migration to the tip of the tail where they dissociated to form terminal neuromasts by 52 hpf (Fig. 3A,H). By contrast, both TB and SB *snail1b* morpholinos reduced the number of deposited neuromasts to three or four and the primordium did not complete its migration by 52 hpf (Fig. 3B,C,H).

The specificity of the effects of TB morpholino was demonstrated by suppressing the morphant phenotype with co-injection of *snail1b* mRNA. Injection of relatively high levels of *snail1b* mRNA

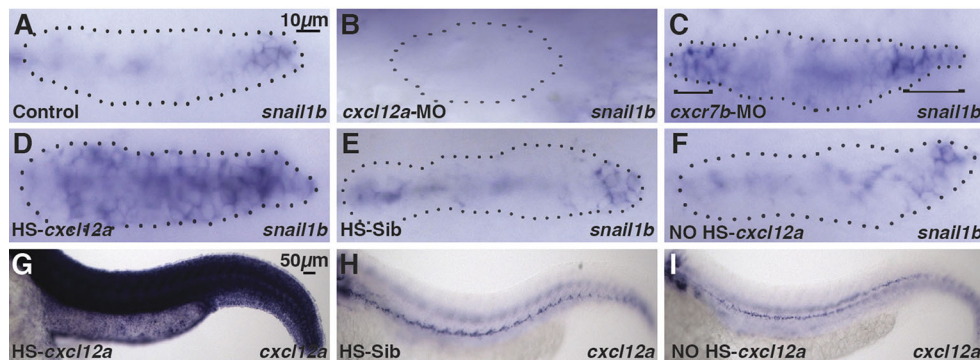


Fig. 2. Cxcl12a promotes expression of *snail1b* in the leading domain. (A,B) *snail1b* expression at the leading end of the primordium in the control embryos (A) and loss of *snail1b* expression following *cxcl12a* knockdown (B). (C) *snail1b* expression at both ends (brackets) following *cxcr7b* knockdown. (D) Broad *snail1b* expression in heat-shocked HS:*cxcl12a* transgenic embryos (HS-*cxcl12a*). (E,F) *snail1b* expression in non-heat-shocked transgenics (NO HS-*cxcl12a*) (E) and in heat-shocked non-transgenic siblings (HS-Sib) (F). (G) *cxcl12a* induction in the embryo following heat shock-induced expression of *cxcl12a* in HS:*cxcl12a* transgenic embryos. (H,I) Lack of *cxcl12a* induction in non-heat-shocked (H) and in heat-shocked non-transgenic siblings (I). $n=20$ for each of two independent experiments. Dotted lines encircle pLL primordia.

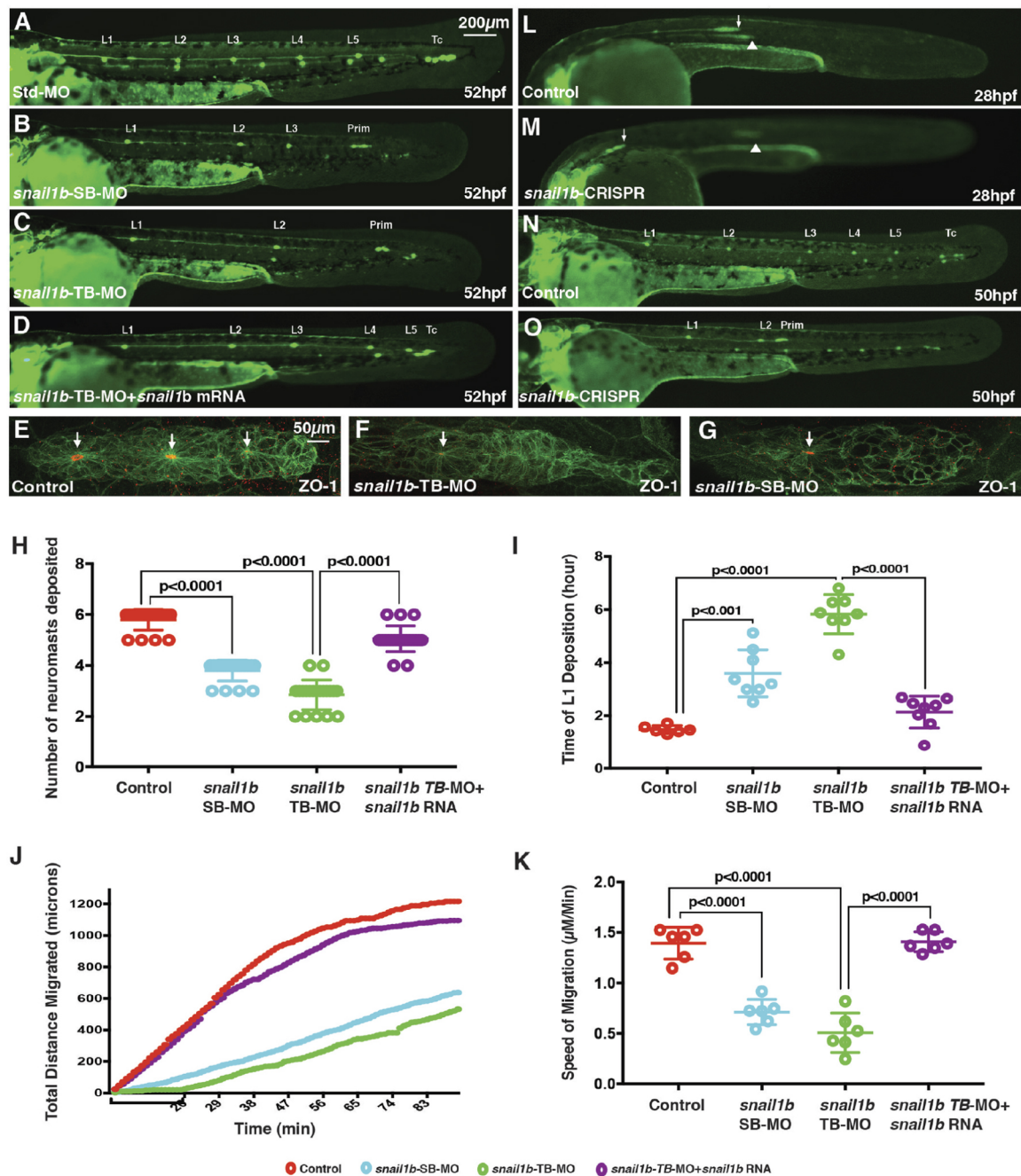


Fig. 3. Delayed neuromast formation and primordium migration following reduction of *snail1b* function. (A-D) The pattern of neuromast deposition visualized in CldnB:lyn-GFP embryos at 52 hpf in control (A), *snail1b* splice-blocking morpholino (SB-MO)-injected embryos (B), *snail1b* translation-blocking morpholino (TB-MO)-injected embryos (C) and *snail1b*-TB morphants co-injected with *snail1b* mRNA (D). (E-G) Expression of ZO-1 (red) in a control embryo (E), a TB morphant (F) and an SB morphant (G). Arrows indicate ZO-1 at apical constriction of proneuromasts. (H) Graphs comparing the number of neuromasts deposited (H) and time of first neuromast (L1) deposition (I) in various experimental conditions. (J) Plot comparing the total distance travelled by the primordium with time in control, SB-MO-injected, TB-MO-injected, and TB-MO and *snail1b* mRNA co-injected embryos. Bracket below the x-axis highlights the delay in initiation of migration in *snail1b* morphants. (K) Comparison of the average migration speed of the primordium. Significance in H, I and K was determined by Student's unpaired *t*-test. In H, I, K, error bars represent standard error of the mean. (L, M) Primordium position (arrow) in a control embryo at 28 hpf (L) and in a *snail1b*-CRISPR-injected embryo (M). Arrow shows primordium on one side with delayed migration, and arrowhead points to slightly out of focus primordium on the contralateral side at a position similar to that in control embryos. (N, O) Pattern of neuromast deposition in a control embryo (N) and an example of a *snail1b*-CRISPR-injected embryo with fewer neuromasts and incomplete primordium migration (O) at 50 hpf. *n*=20 for each of three and two independent morpholino and CRISPR experiments, respectively. Prim, primordium; Tc, terminal cluster.

(200–250 pg) resulted in developmental defects including a shortened body axis, as described previously (data not shown) (Blanco et al., 2007). However, injection of 100 pg *snail1b* mRNA did not cause obvious morphological defects. This concentration

was used to suppress the morphant phenotype. Whereas embryos injected with TB morpholino alone had only three or four deposited neuromasts, co-injection of the TB morpholino with 100 pg *snail1b* mRNA restored the number of deposited neuromasts to an average

of five and the primordium completed its migration with formation of terminal neuromasts by 50 hpf (Fig. 3D,H).

ZO-1 (Tjpl1a – Zebrafish Information Network), which is associated with tight junctions, was examined to determine whether the reduced number of deposited neuromasts was related to a delay in their sequential formation within the migrating primordium. ZO-1 was typically seen associated with the apical constrictions of two relatively mature trailing protoneuromasts and a third most recently formed leading protoneuromast in control primordia. Less prominent localization of ZO-1 was seen in a single relatively immature trailing protoneuromast in the primordia of both TB and SB morpholino-injected embryos (Fig. 3E-G). This confirmed that deposition of fewer neuromasts is related, at least in part, to a delay in their morphogenesis within the migrating primordium.

In addition to depositing fewer neuromasts, time-lapse movies showed that in morphants there was a delay in deposition of the first neuromast (L1) in the morphants; the primordium began its migration following a short delay, and migration was slower (Movie 1, Fig. 3I-K). Furthermore, whereas the control primordia had reached the tail tip, stopped migrating and formed terminal neuromasts by 50 hpf, morphant primordia were still actively migrating and had not formed terminal neuromasts (Movie 1) at 50 hpf. These problems were prevented by co-injecting *snail1b* TB morpholino with *snail1b* mRNA (Movie 2).

We tried to generate homozygous *snail1b* mutants to compare with *snail1b* morphants. F1 progeny from CRISPR/Cas9- and *snail1b* guide RNA-injected G0 fish were identified carrying insertions or deletions expected to result in loss of *snail1b* function (data not shown). However, heterozygous fish carrying these mutations did not produce either functional sperm or eggs and no homozygous mutant progeny could be obtained for analysis. Although their F1 progeny were infertile, key changes observed in *snail1b* morphants were also observed in pLL primordia of some CRISPR/Cas9- and *snail1b* guide RNA-injected G0 embryos (Fig. 3L-O and Fig. 4X-Z). At 28 hpf, in 20/50 G0 embryos, primordia on one side had migrated a shorter distance than on the other side (Fig. 3L,M), suggesting that in this subset of primordia CRISPR-mediated mutations had caused a delay in migration similar to that observed in *snail1b* morphant embryos. Two of these embryos subsequently died, but when the surviving embryos were re-examined at 50 hpf, all of them had fewer neuromasts on one side of the embryo and the primordia had not completed migration (Fig. 3N,O). The observation of such changes, only on one side and in a subset of injected embryos, is consistent with the expected mosaic distribution of cells with effective CRISPR-induced somatic mutations.

Delay in initiation of collective migration is related to the function of *snail1b* in the pLL primordium

The delay in initiation of effective primordium migration in *snail1b* morphants could potentially result from changes in the primordium itself, whereby *snail1b* is expressed in leading cells, and/or from problems in the underlying *snail1b*-expressing horizontal myoseptum cells, which express *cxcl12a* to define the migratory path of the pLL primordium. To distinguish between these possibilities, we first examined the expression of *cxcl12a* at various time points and found no obvious change in the spatiotemporal pattern of *cxcl12a* expression along the horizontal myoseptum in *snail1b* morphants (Fig. S3A-F), suggesting no obvious problem in the differentiation of the cells that define the migratory path. Next, to confirm that the delay in initiating

collective migration is related to a function of *snail1b* in the pLL primordium, rhodamine-dextran labeled cells from uninjected donors were transplanted into *snail1b* morpholino-injected embryos at the 1000-cell stage. Donor cells were placed halfway between the animal pole and the margin in host embryos, where they frequently give rise to ectoderm-derived primordium cells. Embryos were selected in which wild-type cells were only delivered to a primordium on one side of the morphant embryo and the primordium on the other side, composed only of morphant cells, served as a control. Viewing the embryo from the dorsal side allowed us to track migratory behavior of the primordium on the right and left of the embryo simultaneously (Fig. 4A-A"). When wild-type donor cells were successfully transplanted into *snail1b* morphant pLL primordia, they were also often located in the overlying skin, as both primordium and skin cells have neighboring ectodermal origins. However, it was relatively easy to identify morphant primordia with transplanted wild-type cells, as there were no wild-type cells in the underlying horizontal myoseptum cells (Fig. 4B-B"). This is consistent with the relatively distinct spatial separation of prospective primordium cells in the ectoderm, and prospective horizontal myoseptum in the mesoderm at the 1000-cell stage. Transplant experiments showed that 11/13 *snail1b* morphant primordia that had received transplanted wild-type cells migrated further than morphant pLL primordia on the contralateral side that had received no wild-type cells (Fig. 4A-A", Movie 3). In one case, in which a *snail1b* morphant host primordium received donor wild-type cells but did not migrate faster than the contralateral morphant primordium, the wild-type cells were at the trailing end of the primordium, not at the leading end where *snail1b* is expressed (Movie 4). Together, these observations show that problems with migration in *snail1b* morphants have more to do with the function of *snail1b* at the leading end of the primordium and less to do with *snail1b* expression in underlying horizontal myoseptum cells, where it is also expressed.

Loss of *snail1b* results in reciprocal changes in *epcam* and *cdh2* expression

Previous studies have demonstrated that slower migration of axial mesendoderm cells during gastrulation in *snail1b* morphants is related to de-repression of *cdh1* (*cadherin 1*; also known as *e-cadherin*) (Blanco et al., 2007). Although there were no obvious changes in *cdh1* expression in the *snail1b* morphant primordium (data not shown), there were reciprocal changes in the expression of transcripts encoding two other cell adhesion molecules, epithelial cell adhesion molecule (*Epcam*) and *Cdh2* (*cadherin 2*; also known as N-cadherin). *cdh2* and *epcam* are expressed throughout the primordium; however, *cdh2* is most prominent in the leading two thirds of the primordium, whereas *epcam* is expressed in the trailing part in association with maturing protoneuromasts (Fig. 4C,D). However, in *snail1b* morphants *cdh2* expression was reduced, especially in the leading region, whereas, in contrast, *epcam* expression became much more prominent in the leading region (Fig. 4E,F). Co-injection of 100 pg *snail1b* mRNA restored *cdh2* expression and reduced *epcam* expression in the leading part of the primordium of *snail1b* morphants (Fig. 4G,H). Consistent with a role for *snail1b* in repressing *epcam* expression, injection of 100 pg *snail1b* mRNA on its own resulted in an overall reduction in *epcam* (Fig. 4J, Fig. S4B). By contrast, there was no obvious increase in *cdh2* expression following ectopic *snail1b* expression (Fig. 4I, Fig. S4A). Reciprocal changes in *cdh2* and *epcam* were not non-specifically related to slower migration as no obvious change in expression was seen when migratory behavior of the primordium

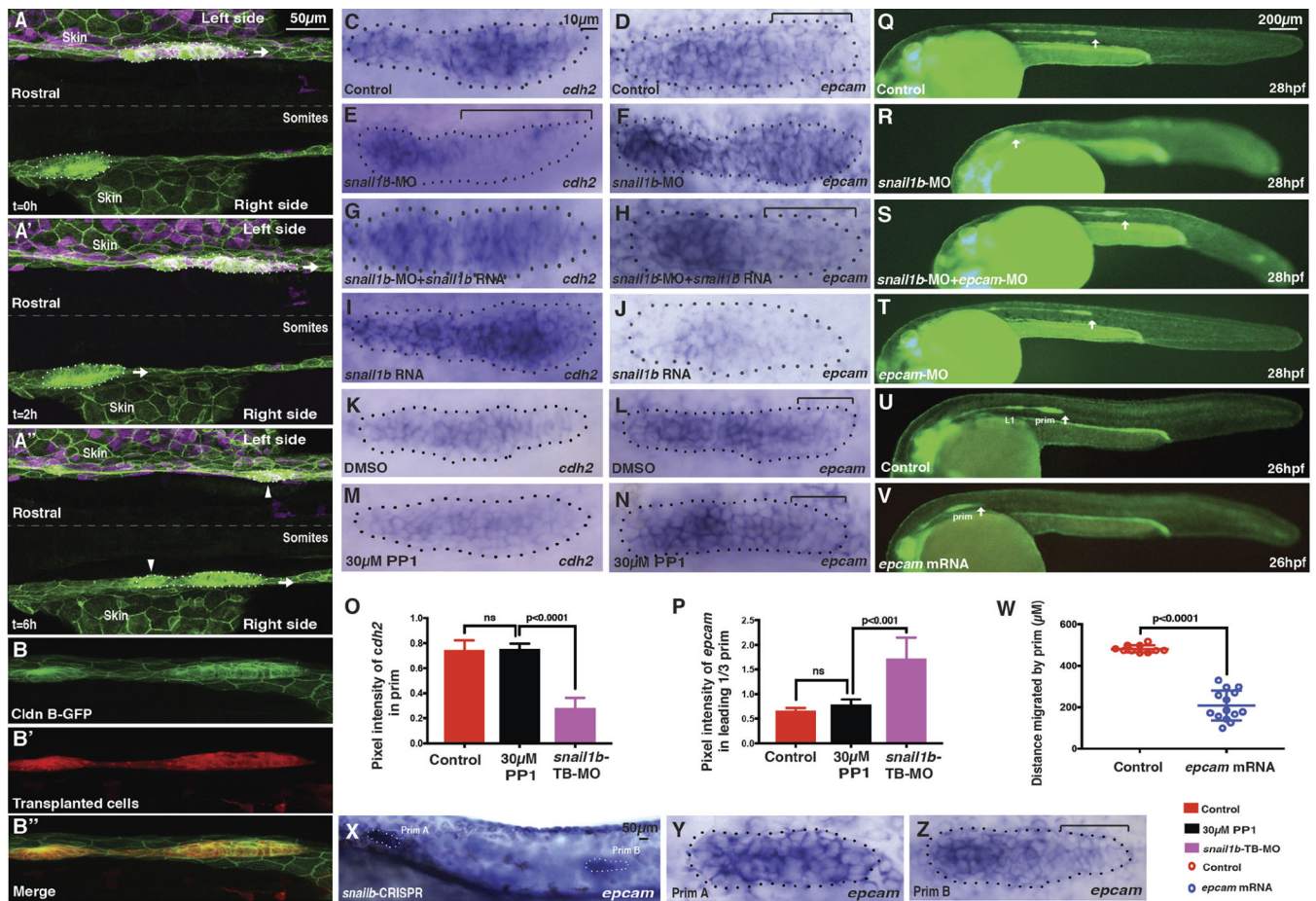


Fig. 4. *Snail1b* is required in the migrating primordium for effective migration and its loss has reciprocal effects on of *cdh2* and *epcam* expression. (A-A'') Stills from a time-lapse movie of pLL primordia migration in *snail1b* morphant embryo (Movie 3) at 0 h (A), 2 h (A') and 6 h (A''). The dorsal view shows the left and right primordia. Transplanted wild-type cells (magenta) are localized in the left primordium and overlying skin but not in underlying horizontal myoseptum. (B-B'') Example of a primordium in a TB-MO-injected *Cldn B:lynGFP* transgenic embryo with transplanted cells from a non-morphant donor embryo but without transplanted cells in the underlying horizontal myoseptum. Transplanted cells are labeled with rhodamine-dextran. (C-J) Expression of *cdh2* and *epcam* in control primordia (C,D), in *snail1b*-TB morphants (E,F), in *snail1b*-TB morphants co-injected with *snail1b* RNA (G,H) and in *snail1b* mRNA-injected embryos (I,J). (K-N) *cdh2* and *epcam* expression in DMSO- and PP1-treated embryos. (O,P) Quantification of *cdh2* and *epcam* expression following inhibition of migration by the Src inhibitor PP1 and in *snail1b* morphants. Error bars represent standard error of the mean. (Q-S) Reversal of slower primordium migration defect in *snail1b* morphants by co-injection of *epcam* morpholinos. Arrow shows position of the primordium. (T) Primordium migration is similar to controls in embryos injected with *epcam*-MO alone. (U,V) Ectopic expression of *epcam* mRNA slows migration of the primordium (prim). (W) Distance migrated by control and *epcam* mRNA-injected embryos. Error bars represent standard error of the mean. (X-Z) *epcam* expression expands into the leading zone of slower migrating primordia of *snail1b* CRISPR-injected embryos. X show a lower magnification of the embryo shown in Y,Z, which show the slower migrating primordium (Prim A) and the contralateral faster migrating primordium (Prim B). The primordium with delayed migration (Y) has expanded *epcam* expression in the leading domain compared with the contralateral side (Z), where there is a lower level of expression in the leading domain. $n=13$ for transplants, $n=25$ for each of two independent experiments for *in situ* hybridization. $n=20$ and 14 for each of two independent experiments of *epcam* rescue and overexpression, respectively. Dotted lines encircle pLL primordia.

was inhibited by exposure to Src kinase inhibitor PP1 (Hanke et al., 1996) (Fig. 4K-P).

To determine whether the expansion of *epcam* expression into the leading zone of the primordium is a crucial change that determines the delay in initiating collective migration we investigated whether partially knocking down *epcam* reduces this delay in *snail1b* morphants. At 28 hpf, the pLL primordium has typically migrated halfway along the length of the yolk extension in control embryos (Fig. 4Q). However, in *snail1b* morphants the primordium is still close to the otic vesicle because of the delay in initiating collective migration (Fig. 4R). However, in 26/30 *snail1b* morphants co-injected with 1.2 ng *epcam* morpholino, there did not appear to be any delay in migration (Fig. 4S), suggesting that expanded *epcam* expression is a significant determinant of delayed collective

migration in *snail1b* morphants. It is important to note that although *epcam* knockdown prevented a migration problem associated with expanded *epcam* expression in *snail1b* morphants, injection of 1.2 ng *epcam* morpholino on its own did not significantly affect either pLL migration (Fig. 4T) or the pattern in which neuromasts were deposited (Fig. S5D-G). It did, however, result in aberrant morphogenesis of otoliths (Fig. S5A-C), recapitulating both the ear phenotype and absence of lateral line phenotype previously described in *epcam* mutants (Slanchev et al., 2009).

Consistent with expanded *epcam* expression having a crucial role in determining delayed primordium migration in *snail1b* morphant embryos, at 26 hpf the primordium had migrated a much shorter distance in embryos injected with 30 pg of *epcam* mRNA compared with uninjected controls (Fig. 4U-W).

As expanded *epcam* expression was a consistent feature of *snail1b* morphant primordia we investigated whether such expanded *epcam* expression was also observed in the subset of primordia that were characterized by slower migration in CRISPR/Cas9- and *snail1b* guide mRNA-injected G0 embryos. All surviving primordia with slower migration scored in the earlier section (Fig. 3L,M) were found to have expanded *epcam* expression (Fig. 4X-Z) supporting the interpretation that this is a key change that accompanies slower/delayed migration when *snail1b* function is lost.

Shrinking of the Wnt system and establishment of Fgf signaling is delayed in *snail1b* morphants

As formation of protoneuromasts is dependent on Fgf signaling, we investigated whether the delay in their formation in *snail1b*

morphants is associated with a delay in the progressive restriction of Wnt signaling to a smaller leading zone and to the stable establishment of the trailing Fgf signaling system. By 26 hpf, Wnt signaling-dependent expression of *lef1* is restricted to a leading domain in control embryos, whereas in *snail1b* morphants, *lef1* expression remains expanded and extends into the trailing zone (Fig. 5A,D). At 35 hpf, the *lef1* expression domain in *snail1b* morphants remains larger than that in controls (Fig. 5B,E). It is nevertheless restricted to a leading zone by this stage. Conversely, although well-established Fgf signaling centers, demarcated by *pea3* expression, were seen in control embryos at 26 hpf, *pea3* expression was either absent or just being initiated at the trailing end of the primordium in *snail1b* TB morphants (Fig. 5G,J). The *pea3* expression domain was, however, well established in *snail1b* morphants by 35 hpf (Fig. 5H,K). The *pea3* expression domain was, however, well established in *snail1b* morphants by 35 hpf (Fig. 5H,K).

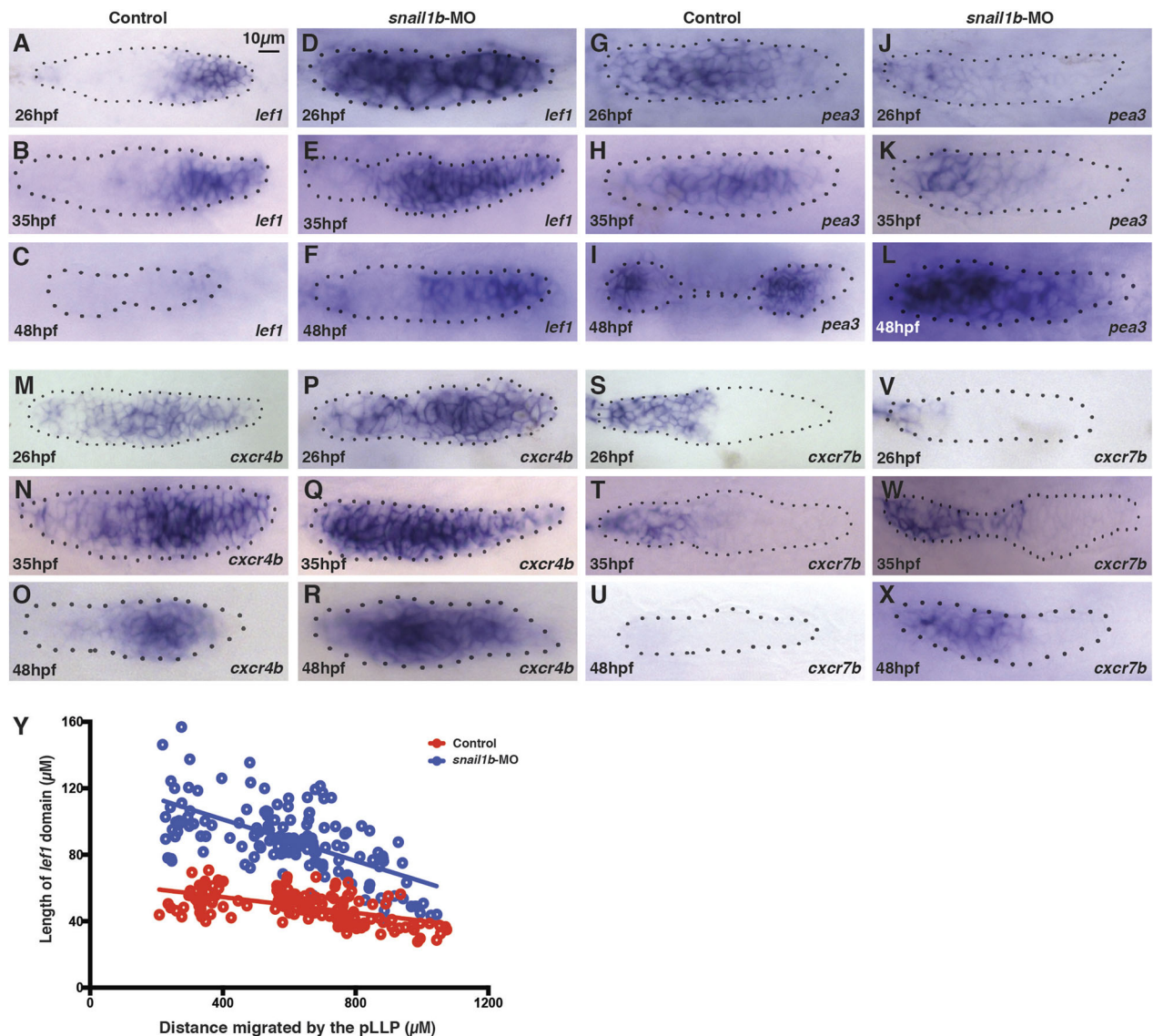


Fig. 5. Delayed Wnt Fgf signaling dynamics in the primordium of *snail1b* morphants. (A-C) Progressive restriction and eventual loss of *lef1* expression in controls from 26 to 48 hpf. (D-F) Delayed restriction and persistent *lef1* expression in *snail1b* morphants. (G-I) *pea3* expression from 26 to 48 hpf in control embryos. (J-L) Delayed establishment and persistent trailing expression of *pea3* expression in *snail1b* morphants. (M-O) *cxcr4b* expression from 26 to 48 hpf in control embryos. (P-R) Broad persistent *cxcr4b* expression in *snail1b* morphants. (S-U) *cxcr7b* expression from 26 to 48 hpf in control embryos. (V-X) Delayed establishment and persistent *cxcr7b* expression in *snail1b* morphants. (Y) Graph of length of the *lef1* expression domain in control and *snail1b*-MO embryos plotted against the distance migrated by the pLL primordium. $n=25$ for each of two independent experiments if not stated in the text, $n=147$ and 144 for control and *snail1b*-MO for the data shown in Y. Dotted lines encircle pLL primordia.

The delay in the shrinking of the leading Wnt system was accompanied by a corresponding delay in the eventual loss of Wnt signaling. In control embryos, the *lef1* expression domain progressively shrinks and is lost in most embryos (18/24) by 48 hpf. However, in *snail1b* morphants *lef1* was still expressed in a relatively broad leading zone at 48 hpf (32/32) (Fig. 5C,F). Similarly, *pea3* expression moves progressively closer to the leading end of the primordium and by 48 hpf in control embryos is associated with the entire primordium, which at this stage has stopped migrating and has resolved to form terminal neuromasts. In *snail1b* morphants, however, the primordium had not resolved to form terminal neuromasts and *pea3* expression was still restricted to a broad trailing zone of the primordium at 48 hpf (Fig. 5I,L). One interpretation of the delay in Wnt and Fgf signaling dynamics in *snail1b* morphants is that the size of the Wnt system reflects its position along the migratory path and the delay in the shrinking of the Wnt system simply reflects the delay in initiating primordium migration. However, plotting the size of the leading Wnt system as a function of the distance travelled by the primordium, rather than as a function of time, showed that shrinking of the Wnt system is delayed, even when one considers the position of the primordium along its migratory path (Fig. 5Y).

The delay in restricting Wnt signaling and establishing a trailing Fgf signaling system was accompanied by a delay in establishment of polarized chemokine receptor expression. *cxc4b*, typically restricted to the leading zone by 26 hpf in control embryos, remained relatively broad in *snail1b* TB morphants (Fig. 5M,P). Similarly, whereas there is normally robust expression of *cxc7b* in a trailing zone of the pLL primordium in control embryos by 26 hpf, its expression was absent or just being initiated in *snail1b* TB morphant embryos (Fig. 5S,V). By 35 hpf, as in control embryos, polarized *cxc7b* expression was established in the trailing part of the primordium in *snail1b* morphants (Fig. 5T,W). However, unlike controls, expression of *cxc4b* remained broad and relatively unpolarized in *snail1b* morphants at 35 hpf and 48 hpf (Fig. 5N,Q,O,R). On the other hand, the delay in the demise of the Wnt system and the resolution of the primordium to form terminal neuromasts was accompanied by a failure to lose *cxc7b* expression in the trailing zone at 48 hpf (Fig. 5U,X). This was accompanied by persistent migratory behavior of the morphant primordium at a time when the control primordium had terminated its migration and resolved to form terminal neuromasts (data not shown).

As shown previously in the context of morphogenesis and migration phenotypes, co-injection of *snail1b* mRNA in *snail1b* morphants prevented the delay in shrinking of the Wnt system and in the establishment of the trailing Fgf signaling system. Although 100 pg *snail1b* mRNA had no obvious effect on expression on its own, co-injection with *snail1b* TB morpholino restored timely restriction of *lef1* expression to a leading zone and the establishment of *pea3* and *cxc7b* expression in the trailing zone by 26 hpf (Fig. S6A-H,M-P). Co-injection of *snail1b* mRNA in the morphants did not, however, prevent aberrant expression of *cxc4b* in the trailing zone (Fig. S7I-L).

Failure of collective migration prevents progressive restriction of the Wnt system

As expression of *snail1b* at the leading end of the primordium is determined by Cxcl12a-dependent chemokine signaling, we investigated whether loss of *cxcl12a* prevents *snail1b* expression and delays restriction of Wnt and establishment of the trailing Fgf signaling systems, as observed in *snail1b* morphants. Examination of *lef1* showed that, whereas *lef1* was restricted to the leading domain at 22 hpf in control embryos (Fig. 6A), *lef1* expression remained broad in *cxcl12a* morphant primordia (Fig. 6B).

Furthermore, a small *pea3* expression domain was established in *cxcl12a* morphants, without delay, at the trailing end of the prospective pLL primordium by 22 hpf (Fig. 6D,E). However, this *pea3* expression domain was in the middle of a broad *lef1* expression domain, which represents a pLL primordium and pLL ganglion that have failed to separate in the absence of effective collective migration (compare Fig. 6B and E). Although a small *pea3* expression domain was established at the trailing end of the prospective pLL primordium in *cxcl12a* morphants, no additional Fgf signaling centers, marked by progressive expansion of *pea3* expression, were established.

Although there were similar delays in shrinking of the Wnt system in *snail1b* morphants and *cxcl12a* morphants, in which *snail1b* expression in the primordium is indirectly lost, there were important differences. Whereas progressive restriction of the Wnt system was delayed in *snail1b* morphants, it was permanently blocked in *cxcl12a* morphants, in which caudal migration is not just delayed but permanently lost. This suggested that the severity of problems associated with the failure to progressively restrict the domain of Wnt activity correlated with the delay or complete failure

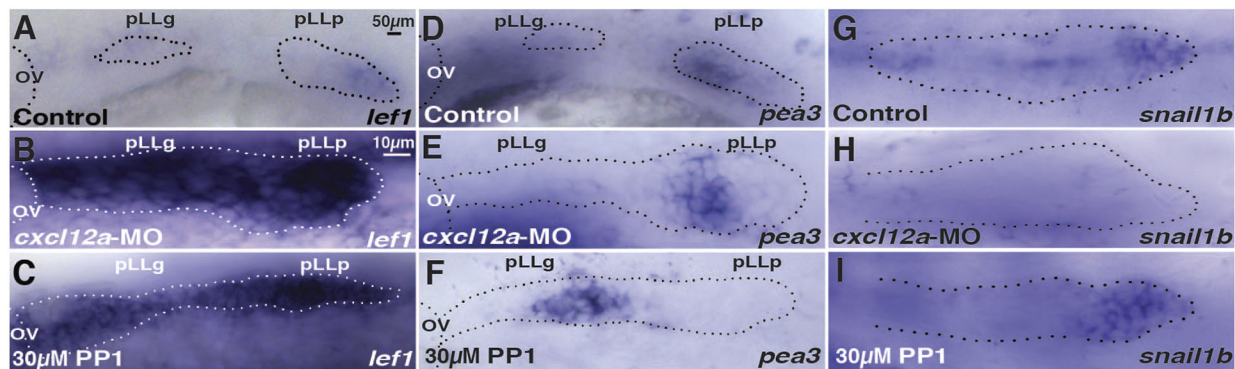


Fig. 6. Delayed Wnt Fgf signaling dynamics in stalled primordia. (A) In control embryos, the primordium (pLLp) migrates and separates from the pLL ganglion (pLLg) by 22 hpf and *lef1* expression is restricted to the leading domain. (B,C) With migration inhibited in *cxcl12a* morphants and PP1-treated embryos, the primordium remains juxtaposed with the pLLg and *lef1* expression remains broad. (D) *pea3* expression at the trailing end of the primordium in controls at 22 hpf. (E,F) The *pea3* expression domain is still at the trailing end of the prospective primordium in the absence of migration; however, the *pea3* domain is in the middle of a broad *lef1*-expressing domain, which now represents the juxtaposed primordium and the pLLg. (G-I) *snail1b* expression in control, *cxcl12a* morphant and PP1-treated primordia at 22 hpf. OV, otic vesicle. $n=25$ for each of two independent experiments. Dotted lines encircle pLL primordia.

of caudal migration, not specifically with loss of *snail1b* function. To determine whether loss of migratory behavior causes a delay in restriction of Wnt signaling and sequential formation of Fgf signaling-dependent protoneuromasts, we examined *lef1* and *pea3* expression in embryos in which collective migration was inhibited with a Src kinase inhibitor, PP1. Exposure of embryos to 30 μ M PP1 at 18 hpf stalled migration of the primordium. As in *snail1b* and *cxcl12a* morphants, restriction of *lef1* expression to the leading domain and establishment of expanded *pea3* expression in the trailing domain was delayed (Fig. 6C,F). Nevertheless, in this context, chemokine-dependent expression of *snail1b* in leading cells was not affected (Fig. 6G-I), suggesting that the similar phenotype seen in *cxcl12a* morphants was not specifically dependent on either *cxcl12a* or chemokine signaling-dependent expression of *snail1b*. Instead, these observations suggest that the delay in sequential formation of Fgf signaling-dependent protoneuromasts is likely to be related, at least in part, to the delay in initiation of effective collective migration of the primordium.

DISCUSSION

Fgf signaling in the trailing part of the primordium determines the reorganization of sequential groups of cells as epithelial rosettes to form protoneuromasts, whereas Wnt signaling is thought to maintain the relatively mesenchymal morphology of leading cells, where it dominates (Aman and Piotrowski, 2008; Lecaudey et al., 2008; Nechiporuk and Raible, 2008). However, how Wnt signaling determines mesenchymal morphology was not clear. Our discovery that *snail1b* is expressed in leading cells led us to speculate that its expression might be determined by Wnt signaling and that, as a factor known for its role in promoting EMT (Barrallo-Gimeno and Nieto, 2005; Dang et al., 2011; Lamouille et al., 2014), it might determine mesenchymal morphology of leading cells. However, our analysis revealed that Wnt signaling does not determine *snail1b* expression in the leading zone. Instead, its expression in the leading zone is promoted by chemokine signals first encountered by leading cells of the primordium (Fig. 7A), whereas Fgf signaling prevents *snail1b* expression in trailing cells (Fig. 7B). The effect of knocking down *snail1b* function was also not what we expected. It did not compromise the ability of leading cells to adopt a mesenchymal morphology. Instead, sequential morphogenesis of epithelial rosettes associated with formation of protoneuromasts in the trailing domain was delayed in *snail1b* morphants (Fig. 7C). Our analysis revealed, however, that the delay in protoneuromast formation is not related to a specific role of *Snail1b* in morphogenesis of epithelial rosettes. Instead, it is indirectly related to the role of *Snail1b* in helping to initiate effective collective migration of the primordium, a role consistent with its previously described role in promoting cell movement (Barrallo-Gimeno and Nieto, 2005). Interestingly, we found that other manipulations that prevent effective primordium migration also cause a similar delay in sequential formation of Fgf signaling centers, associated protoneuromasts and shrinking of the leading Wnt system. These observations, together, reveal an unexpected role for collective migration of the primordium in kick-starting sequential formation of additional protoneuromasts. Finally, we showed that problems in initiating collective migration in the primordium may, at least in part, be related to aberrant expansion of *epcam* into the leading zone and/or the loss of *cdh2* expression from the leading zone of the primordium following knockdown of *snail1b* function.

Horizontal myoseptum cells, located caudal to the recently formed primordium, secrete Cxcl12a and determine a migratory response in

Cxcr4b-expressing cells at the caudal end of the primordium, to initiate and bias the initial direction of primordium migration (Dambly-Chaudière et al., 2007). This study now shows that, in addition to providing a directionally biased guidance cue to leading cells, Cxcl12a initiates *snail1b* expression in cells at the caudal end of the primordium. This helps to kick-start effective collective migration of the entire primordium. Though the initial exposure of the primordium to Cxcl12a is asymmetric, once the primordium is migrating over the horizontal myoseptum, along the path defined by *cxcl12a* expression, it is exposed at both its leading and trailing ends to Cxcl12. At this stage, establishment of Fgf signaling in the trailing end of the primordium helps to restrict *snail1b* expression to the leading end of the primordium, as loss of Fgf signaling allows *snail1b* expression to expand into the trailing zone.

The failure to initiate effective collective migration of the pLL primordium in *snail1b* morphants has additional consequences related to sequential formation of protoneuromasts and associated changes in Wnt and Fgf signaling in the primordium. *snail1b* morphants are associated with a delay in formation of an expanding Fgf signaling system at the trailing end of the pLL primordium and in the accompanying restriction of the initially broad Wnt signaling system to a progressively smaller leading zone in the primordium. Interestingly, inhibition of collective migration by other manipulations, including knockdown of *cxcl12a* or exposure to the Src kinase inhibitor PP1, caused a similar delay in progressive restriction of the Wnt system to a smaller leading zone and in establishment of additional Fgf signaling centers associated with formation of protoneuromasts. Although it remains unclear how sequential formation of additional protoneuromasts is related to collective migration, one simple possibility is that migratory behavior alters the shape of the primordium. In the absence of collective migration all the cells in the primordium tend to coalesce to form one or two relatively large unstable epithelial rosettes. Initiation of collective migration alters the shape of the primordium by stretching the initially large ellipsoid collection into a longer column of cells. In the context of self-organizing mechanisms that might impose a minimum distance between sequentially formed epithelial rosettes, stretching the primordium into a longer column following the effective initiation of collective migration may be all it takes to initiate formation of additional protoneuromasts. This hypothesis will be explored in future studies.

Understanding of the dynamics of Wnt and Fgf signaling in the pLL primordium has relied on examining genes like *lef1* and *pea3*, expression of which is determined by Wnt and Fgf signaling, respectively. The discovery that *snail1b* expression is determined by *cxcl12a*-mediated chemokine signaling now provides an avenue for examining the pattern of chemokine signaling in the primordium. Previous studies suggested that polarized expression of chemokine-responsive Cxcr4b and chemokine-unresponsive Cxcr7b at leading and trailing ends of the primordium, respectively, determine a polarized response of the primordium to Cxcl12a. Furthermore, binding, internalization and degradation of Cxcl12a bound to the Cxcr7b receptor contributes to generation of a local gradient of chemokine availability, which facilitates unidirectional collective migration of the primordium. Consistent with this suggestion, chemokine signaling-dependent expression of *snail1b* is normally only observed in leading cells of the primordium. However, when *cxcr7b* is knocked down, the response to Cxcl12a is no longer polarized and *snail1b* expression is observed at both ends of the primordium.

A significant challenge we faced in this study is that we were unable to breed heterozygous fish with *snail1b* CRISPR/Cas9-mediated

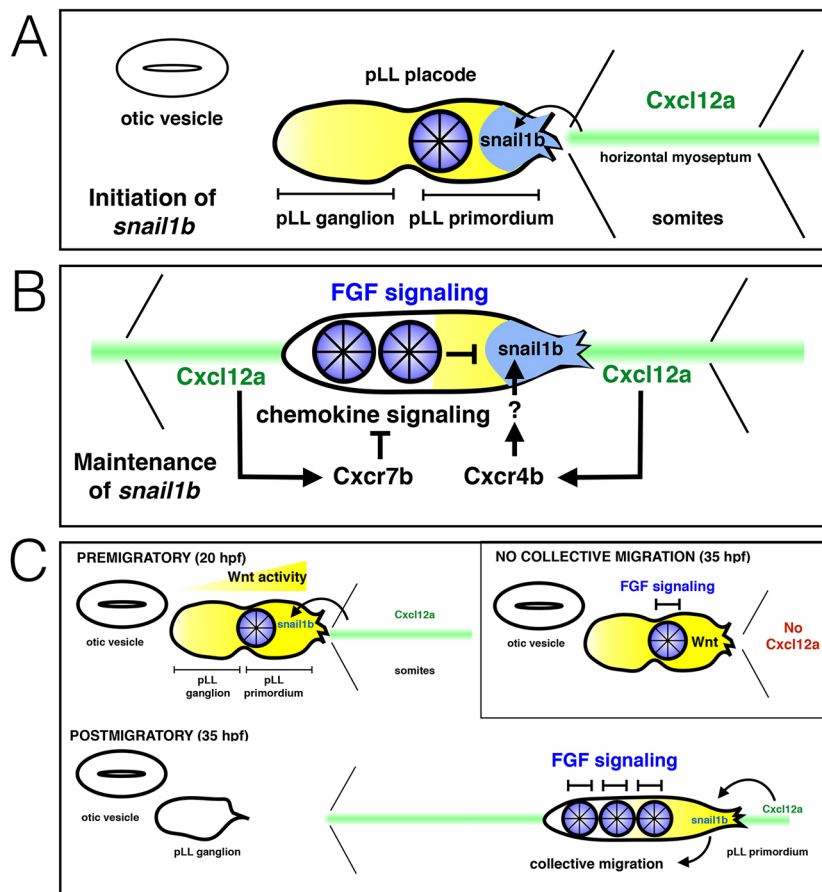


Fig. 7. Polarization and initiation of migration in pLL primordium. (A) *Cxcl12a* (green stripe) initiates *snail1b* expression at the caudal end of the prospective pLL primordium. (B) *snail1b* expression is maintained by *Cxcr4b*-mediated chemokine signaling at the leading end, and *Cxcr7b* inhibits chemokine signaling at the trailing end. *snail1b* expression is also inhibited by Fgf signaling (blue) in the trailing domain. (C) Before migration begins, an Fgf signaling center forms at the boundary of the pLL primordium and pLL ganglion. In the absence of migration, no additional Fgf signaling centers form (inset). Initiation of migration allows sequential formation of additional Fgf signaling centers and shrinking of the leading Wnt-active domain (yellow) (bottom panel).

mutations. Consequently, we have had to rely on morphant phenotypes for our conclusions. There has been considerable debate about the strength of conclusions that are based on morphant studies (Eisen and Smith, 2008; Stainier et al., 2017). Nevertheless, there are many reasons to be confident of key conclusions made in this study. First, similar phenotypes were observed with independent splice-blocking and translation-blocking *snail1b* morpholinos. Second, delays in initiating migration and in sequential formation of protoneuromasts were suppressed or reversed by co-injecting morpholinos with low levels of *snail1b* mRNA. Similarly, changes in gene expression, which account for the observed deficits in migration and formation of protoneuromasts in the *snail1b* morphants, were reversed by co-injection of *snail1b* mRNA. Third, complementary changes in the pattern of gene expression were induced by loss-of-function and gain-of-function experiments. For example, *snail1b* knockdown resulted in *epcam* expanding into the leading zone, where *snail1b* is normally expressed, and ectopic expression of *snail1b* mRNA resulted in suppression of *epcam* expression. Together, these observations provide strong support to conclusions based on the analysis of *snail1b* morphants.

In conclusion, this study has provided a fresh perspective on events associated with formation of the pLL primordium, initiation of polarized caudal migration and sequential protoneuromast formation within the migrating primordium. In addition to initiating polarized migratory behavior of leading cells, the chemokine *Cxcl12a* triggers *snail1b* expression in cells at the leading end of the pLL primordium, which helps to initiate collective migration of the pLL primordium (Fig. 7A). Furthermore, prior to

the initiation of effective collective migration and separation of the rostral pLL ganglion cells from caudal pLL primordium, there is broad Wnt signaling activity across the entire pLL placode. As a boundary between a rostral pLL ganglion and the caudal pLL primordium compartment forms within the pLL placode, an Fgf signaling center and the first protoneuromast is established at this boundary at the trailing end of the prospective pLL primordium (Fig. 7A). Initiation of collective migration then has an important impact on the subsequent dynamics of Wnt and Fgf signaling in the pLL primordium: as collective migration is initiated and the primordium moves away, leaving the pLL ganglion cells in its wake, additional Fgf signaling centers and protoneuromasts form in the pLL primordium. Furthermore, Fgf signaling in the trailing zone helps to restrict *snail1b* expression to the leading zone (Fig. 7B,C). Establishment of additional Fgf-dependent protoneuromasts is accompanied by progressive shrinking of the initially broad system of Wnt activity. In the absence of effective collective migration, additional protoneuromast do not form and the Wnt system remains broad and does not shrink in a timely manner (Fig. 7C, inset). We expect future studies to help define more clearly how *Snail1b* determines the timely initiation of collective migration and how this, in turn, facilitates sequential formation of protoneuromasts.

MATERIALS AND METHODS

Fish maintenance and zebrafish strains

Danio rerio were maintained under standard conditions. Embryos were staged according to Kimmel et al. (1995). *Tg[cldnb:lynGFP]* (Haas and Gilmour, 2006), *Tg[hsDKK1b]* (Stoick-Cooper et al., 2007), *Tg[hsp70l:dnfgfr1-EGFP]/pd1* (Lee et al., 2005) and *Tg[hsp:cxcl12a]* (Knaut et al., 2005)

were previously described. Heat shock was carried out at 37.5°C for 40 min. Embryos were incubated with 10 µm SU5402 (Tocris) or 5 µm BIO (Calbiochem) from 26 hpf until fixation, or with 30 µm PP1 (Sigma) from 18 hpf until fixation at 22 hpf. Drugs were made up in DMSO, and control embryos were incubated for similar periods in DMSO alone. Experiments were carried out in accordance with National Institute of Child Health and Human Development Animal Care and Use Committee Protocol Number 15-039.

Morpholino (MO) injections

All MOs were obtained from Gene Tools LLC. MOs used were (5'-3'): *snail1b*-MO1, TGCAAATATCCCCTCGAACTTCAG (Blanco et al., 2007); *snail1b*-SB, CCGTCTGGGAAGAGATCACTTAA; *cxcl12a*-MO1, TTGAGATCCATGTTTGAGTGTGAA (Boldajipour et al., 2008); *cxc7b*-MO2, TCATTACGTTCACTCATCTTGC (Dambly-Chaudière et al., 2007); *epcam*-MO, ACTAAACCTTCATTGTGAGCGAGA (Villablanca et al., 2006). All the MOs were injected at the single-cell stage with co-injection of 1.5 ng of p53-MO (Robu et al., 2007). Standard control MO (CCTCTTACCTCAGTTACAAATTATA; Gene Tools LLC) was injected at the same concentration as the test. Statistical significance was determined by unpaired Student's *t*-test.

Whole-mount *in situ* hybridization and immunohistochemistry

Embryo were fixed in 4% paraformaldehyde (PFA) overnight and dehydrated in methanol for 1 h at -30°C. The embryos were rehydrated, treated with proteinase-K and re-fixed with 4% PFA. Pre-hybridization and hybridization were carried out at 67°C for *snail1b* and 65°C for rest of the probes. RNA probes were synthesized using a DIG labeling kit (Roche, 11175025910). Samples were hybridized overnight with RNA probes and color was developed using BCIP/NBT substrate (Roche, 11383221001, 11383213001). For immunohistochemistry, embryos were fixed in 4% PFA overnight and blocked in PBT (phosphate-buffered saline with 0.1% Tween 20) with 5% goat serum. Antibodies were incubated in the same buffer overnight with anti-GFP (Abcam, ab13970; 1:1000) and anti-ZO1 (Thermo Fisher Scientific, 33-9100; 1:500). Embryos were washed with PBT and incubated with respective secondary antibodies [goat anti-chicken-488 (Invitrogen, A-11039; 1:500) and goat anti-mouse-568 (Invitrogen, A-11031; 1:500)] and imaged on a Leica SP5 confocal microscope.

Time-lapse recordings

For time-lapse acquisition, *Tg[cldnB:lynGFP]* embryos were anesthetized at ~20 hpf in 600 µm Tricaine (Sigma) and mounted in 0.8% low melting agarose (Nusieve GTG, Lonza) in a glass-bottomed chamber slides (Nunc). Movies were acquired until 48 hpf at intervals of 5 min using an inverted Leica SP5 confocal microscope with 10× lens. The data were analyzed using ImageJ (Rasband, 1997-2016).

Acknowledgements

We thank Angela Nieto for the *snail1b* mRNA clone. We thank Chitnis lab members for critical comments.

Competing interests

The authors declare no competing or financial interests.

Author contributions

Conceptualization: U.M.N., A.B.C.; Methodology: U.M.N., D.D.N., A.B.C.; Validation: U.M.N., D.D.N.; Formal analysis: U.M.N., D.D.N., A.B.C.; Investigation: U.M.N., D.D.N., A.B.C.; Data curation: U.M.N.; Writing - original draft: U.M.N., D.D.N., A.B.C.; Writing - review & editing: U.M.N., D.D.N., A.B.C.; Visualization: U.M.N., D.D.N., A.B.C.; Supervision: A.B.C.; Project administration: A.B.C.; Funding acquisition: A.B.C.

Funding

This project was funded by the intramural program of the Eunice Kennedy Shriver National Institute of Child Health and Human Development (HD001012). Deposited in PMC for release after 12 months.

Supplementary information

Supplementary information available online at <http://dev.biologists.org/lookup/doi/10.1242/dev.162453.supplemental>

References

- Aman, A. and Piotrowski, T. (2008). Wnt/beta-catenin and Fgf signaling control collective cell migration by restricting chemokine receptor expression. *Dev. Cell* **15**, 749-761.
- Balabanian, K., Lagane, B., Infantino, S., Chow, K. Y. C., Harriague, J., Moepps, B., Arenzana-Seisdedos, F., Thelen, M. and Bachelier, F. (2005). The chemokine SDF-1/CXCL12 binds to and signals through the orphan receptor RDC1 in T lymphocytes. *J. Biol. Chem.* **280**, 35760-35766.
- Barrallo-Gimeno, A. and Nieto, M. A. (2005). The Snail genes as inducers of cell movement and survival: implications in development and cancer. *Development* **132**, 3151-3161.
- Blanco, M. J., Barrallo-Gimeno, A., Acloque, H., Reyes, A. E., Tada, M., Allende, M. L., Mayor, R. and Nieto, M. A. (2007). Snail1a and Snail1b cooperate in the anterior migration of the axial mesendoderm in the zebrafish embryo. *Development* **134**, 4073-4081.
- Boldajipour, B., Mahabaleshwar, H., Kardash, E., Reichman-Fried, M., Blaser, H., Minina, S., Wilson, D., Xu, Q. and Raz, E. (2008). Control of chemokine-guided cell migration by ligand sequestration. *Cell* **132**, 463-473.
- Coombs, S. and Montgomery, J. C. (1999). The enigmatic lateral line system. In *Comparative Hearing: Fish and Amphibians* (ed. R. R. Fay and A. N. Popper), pp. 319-362. New York: Springer-Verlag.
- Dalle Nogare, D. and Chitnis, A. B. (2017). A framework for understanding morphogenesis and migration of the zebrafish posterior lateral line primordium. *Mech. Dev.* **148**, 69-78.
- Dambly-Chaudière, C., Cubedo, N. and Ghysen, A. (2007). Control of cell migration in the development of the posterior lateral line: antagonistic interactions between the chemokine receptors CXCR4 and CXCR7/RDC1. *BMC Dev. Biol.* **7**, 23.
- Dang, H., Ding, W., Emerson, D. and Rountree, C. B. (2011). Snail1 induces epithelial-to-mesenchymal transition and tumor initiating stem cell characteristics. *BMC Cancer* **11**, 396.
- Donà, E., Barry, J. D., Valentin, G., Quirin, C., Khmelinskii, A., Kunze, A., Durdu, S., Newton, L. R., Fernandez-Minan, A., Huber, W. et al. (2013). Directional tissue migration through a self-generated chemokine gradient. *Nature* **503**, 285-289.
- Eisen, J. S. and Smith, J. C. (2008). Controlling morpholino experiments: don't stop making antisense. *Development* **135**, 1735-1743.
- Ghysen, A. and Dambly-Chaudière, C. (2007). The lateral line microcosmos. *Genes Dev.* **21**, 2118-2130.
- Graham, G. J. (2009). D6 and the atypical chemokine receptor family: novel regulators of immune and inflammatory processes. *Eur. J. Immunol.* **39**, 342-351.
- Haas, P. and Gilmour, D. (2006). Chemokine signaling mediates self-organizing tissue migration in the zebrafish lateral line. *Dev. Cell* **10**, 673-680.
- Hanke, J. H., Gardner, J. P., Dow, R. L., Changelian, P. S., Brissette, W. H., Weringer, E. J., Pollok, B. A. and Connelly, P. A. (1996). Discovery of a novel, potent, and Src family-selective tyrosine kinase inhibitor. Study of Lck- and FynT-dependent T cell activation. *J. Biol. Chem.* **271**, 695-701.
- Itoh, M. and Chitnis, A. B. (2001). Expression of proneural and neurogenic genes in the zebrafish lateral line primordium correlates with selection of hair cell fate in neuromasts. *Mech. Dev.* **102**, 263-266.
- Jiang, L., Romero-Carvajal, A., Haug, J. S., Seidel, C. W. and Piotrowski, T. (2014). Gene-expression analysis of hair cell regeneration in the zebrafish lateral line. *Proc. Natl. Acad. Sci. USA* **111**, E1383-E1392.
- Kimmel, C. B., Ballard, W. W., Kimmel, S. R., Ullmann, B. and Schilling, T. F. (1995). Stages of embryonic development of the zebrafish. *Dev. Dyn.* **203**, 253-310.
- Knauf, H., Blader, P., Strähle, U. and Schier, A. F. (2005). Assembly of trigeminal sensory ganglia by chemokine signaling. *Neuron* **47**, 653-666.
- Lamouille, S., Xu, J. and Derynck, R. (2014). Molecular mechanisms of epithelial-mesenchymal transition. *Nat. Rev. Mol. Cell Biol.* **15**, 178-196.
- Lecaudey, V., Cakan-Akdogan, G., Norton, W. H. J. and Gilmour, D. (2008). Dynamic Fgf signaling couples morphogenesis and migration in the zebrafish lateral line primordium. *Development* **135**, 2695-2705.
- Lee, Y., Grill, S., Sanchez, A., Murphy-Ryan, M. and Poss, K. D. (2005). Fgf signaling instructs position-dependent growth rate during zebrafish fin regeneration. *Development* **132**, 5173-5183.
- Matsuda, M. and Chitnis, A. B. (2010). Atoh1a expression must be restricted by Notch signaling for effective morphogenesis of the posterior lateral line primordium in zebrafish. *Development* **137**, 3477-3487.
- Matsuda, M., Nogare, D. D., Somers, K., Martin, K., Wang, C. and Chitnis, A. B. (2013). Lef1 regulates Dusp6 to influence neuromast formation and spacing in the zebrafish posterior lateral line primordium. *Development* **140**, 2387-2397.
- Meijer, L., Skaltsounis, A.-L., Magiatis, P., Polychronopoulos, P., Knockaert, M., Leost, M., Ryan, X. P., Vonica, C. A., Brivanlou, A., Dajani, R. et al. (2003). GSK-3-selective inhibitors derived from Tyrian purple indirubins. *Chem. Biol.* **10**, 1255-1266.
- Mohammadi, M., McMahon, G., Sun, L., Tang, C., Hirth, P., Yeh, B. K., Hubbard, S. R. and Schlessinger, J. (1997). Structures of the tyrosine kinase domain of fibroblast growth factor receptor in complex with inhibitors. *Science* **276**, 955-960.
- Nechiporuk, A. and Raible, D. W. (2008). FGF-dependent mechanosensory organ patterning in zebrafish. *Science* **320**, 1774-1777.

- Rasband, W. S. (1997-2016). *ImageJ*. Bethesda, Maryland, USA: U.S. National Institutes of Health.
- Robu, M. E., Larson, J. D., Nasevicius, A., Beiraghi, S., Brenner, C., Farber, S. A. and Ekker, S. C. (2007). p53 activation by knockdown technologies. *PLoS Genet.* **3**, e78.
- Sapède, D., Rossel, M., Dambly-Chaudière, C. and Ghysen, A. (2005). Role of SDF1 chemokine in the development of lateral line efferent and facial motor neurons. *Proc. Natl. Acad. Sci. USA* **102**, 1714-1718.
- Sarrazin, A. F., Nunez, V. A., Sapède, D., Tassin, V., Dambly-Chaudière, C. and Ghysen, A. (2010). Origin and early development of the posterior lateral line system of zebrafish. *J. Neurosci.* **30**, 8234-8244.
- Slanchev, K., Carney, T. J., Stemmler, M. P., Koschorz, B., Amsterdam, A., Schwarz, H. and Hammerschmidt, M. (2009). The epithelial cell adhesion molecule EpCAM is required for epithelial morphogenesis and integrity during zebrafish epiboly and skin development. *PLoS Genet.* **5**, e1000563.
- Stainier, D. Y. R., Raz, E., Lawson, N. D., Ekker, S. C., Burdine, R. D., Eisen, J. S., Ingham, P. W., Schulte-Merker, S., Yelon, D., Weinstein, B. M. et al. (2017). Guidelines for morpholino use in zebrafish. *PLoS Genet.* **13**, e1007000.
- Stoick-Cooper, C. L., Weidinger, G., Riehle, K. J., Hubbert, C., Major, M. B., Fausto, N. and Moon, R. T. (2007). Distinct Wnt signaling pathways have opposing roles in appendage regeneration. *Development* **134**, 479-489.
- Valdivia, L. E., Young, R. M., Hawkins, T. A., Stickney, H. L., Cavodeassi, F., Schwarz, Q., Pullin, L. M., Villegas, R., Moro, E., Argenton, F. et al. (2011). Lef1-dependent Wnt/beta-catenin signalling drives the proliferative engine that maintains tissue homeostasis during lateral line development. *Development* **138**, 3931-3941.
- Valentin, G., Haas, P. and Gilmour, D. (2007). The chemokine SDF1a coordinates tissue migration through the spatially restricted activation of Cxcr7 and Cxcr4b. *Curr. Biol.* **17**, 1026-1031.
- Venkiteswaran, G., Lewellis, S. W., Wang, J., Reynolds, E., Nicholson, C. and Knaut, H. (2013). Generation and dynamics of an endogenous, self-generated signaling gradient across a migrating tissue. *Cell* **155**, 674-687.
- Villablanca, E. J., Renucci, A., Sapède, D., Lec, V., Soubiran, F., Sandoval, P. C., Dambly-Chaudière, C., Ghysen, A. and Allende, M. L. (2006). Control of cell migration in the zebrafish lateral line: implication of the gene 'tumour-associated calcium signal transducer,' *tacstd*. *Dev. Dyn.* **235**, 1578-1588.

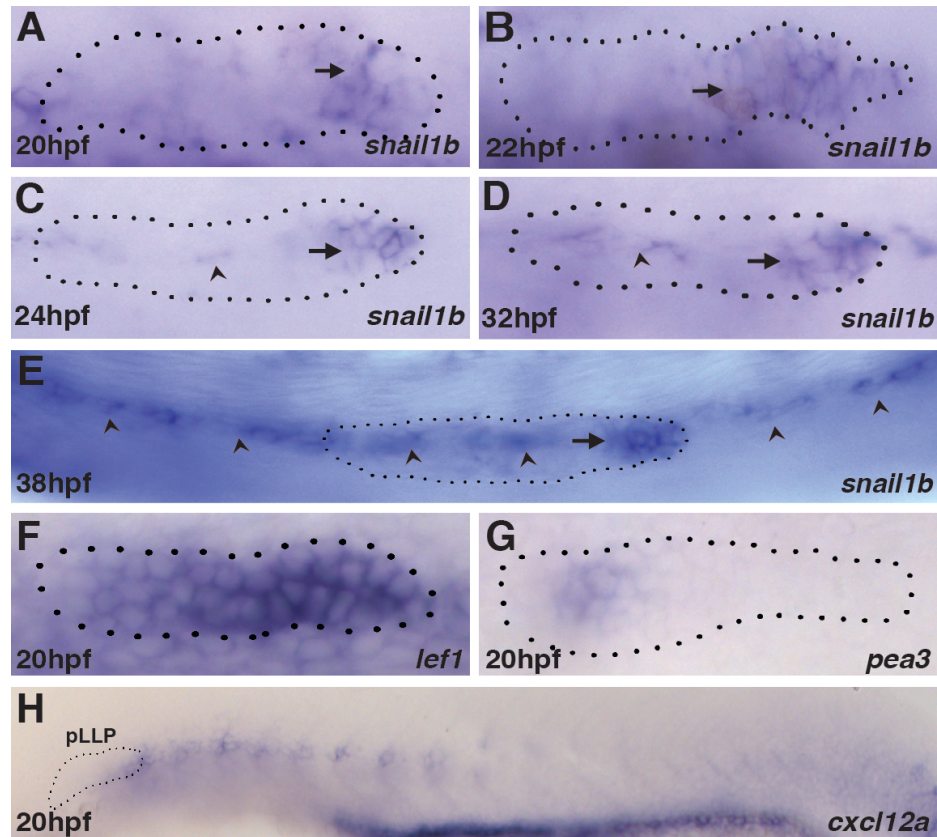


Fig.S1: *snail1b* expression in the leading domain (arrow) at (A) 20hpf, (B) 22hpf, (C) 24hpf (D) 32hpf and (E) 38hpf. arrow heads in C-E show *snail1b* expression in the underlying cells of the horizontal myospetum. (F) At 20hpf, Wnt-dependent *lef1* expression is broad and, (G) FGF-dependent *pea3* has not been effectively established. (H) However, at 20hpf the primordium is only exposed to *cxcl12a* at its caudal end.

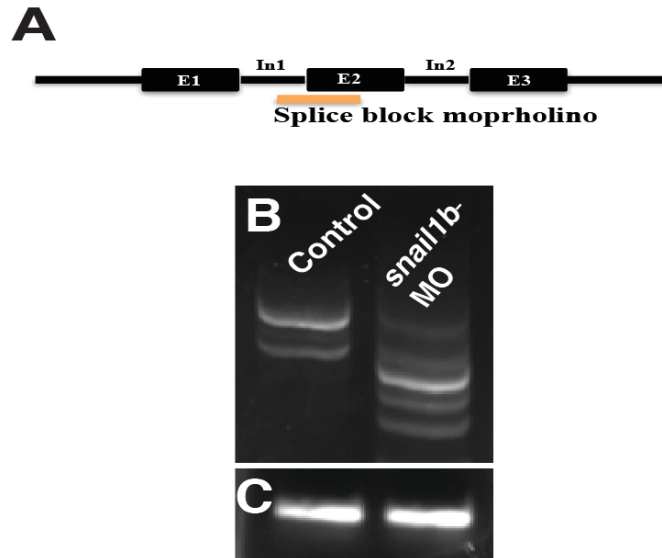


Fig.S2: Splice block *snail1b*-MO. (A) cartoon showing the SB target site of *snail1b*-MO. (B) RT-PCR products of control and *snail1b*-MO. (C) L-24 internal control.

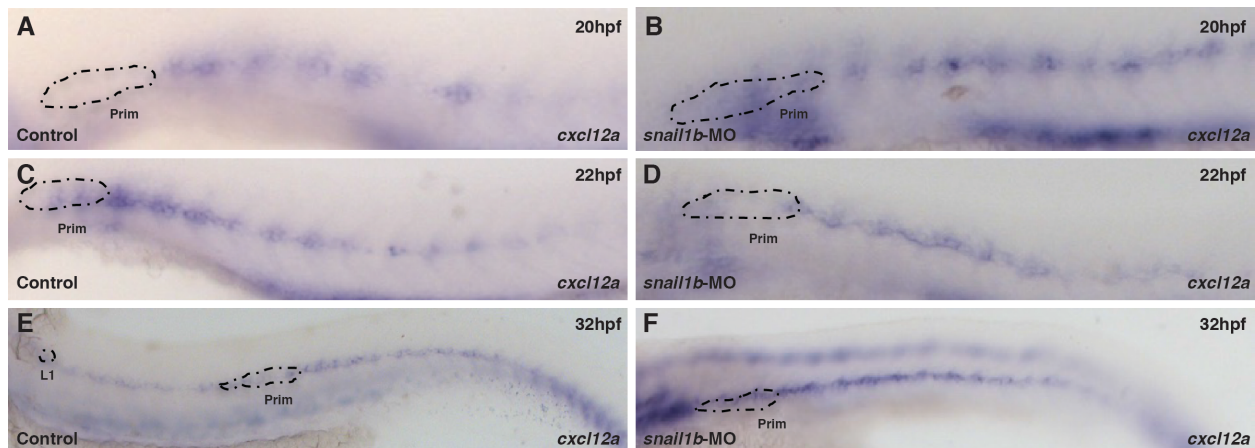


Fig.S3: The delay in initiation of primordium migration in *snail1b* morphants is not due to aberrant *cxcl12a* expression by underlying *snail1b*-expressing horizontal myoseptum cells. *cxcl12a* begins to express on the horizontal myoseptum at 20hpf (A) and it forms a stipe over the entire embryo by 22hpf (C) and continues to express at 32hpf (E) in controls. *snail1b* morphants have similar spatiotemporal pattern of *cxcl12a* expression (B,D,F).

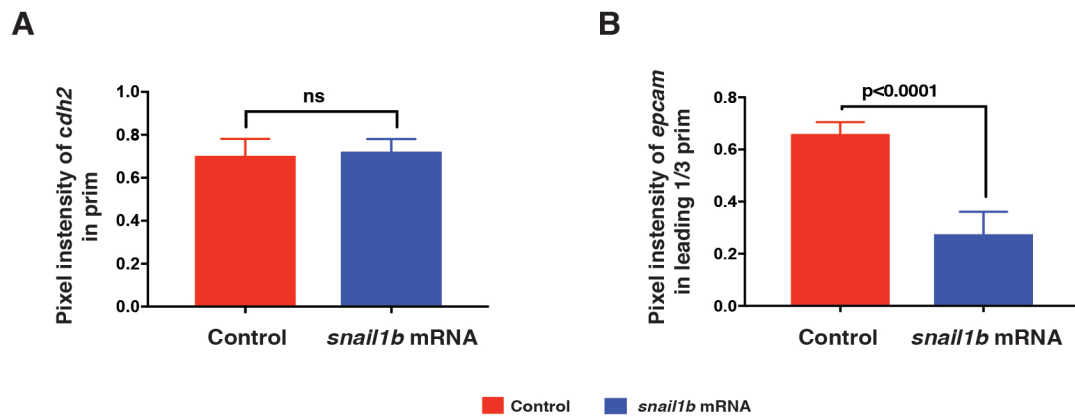


Fig.S4. Quantification of *cdh2* (A) and *epcam* (B) expression in control and *snail1b* mRNA injected embryos. Prim is primordium, error bars represent standard error of the mean

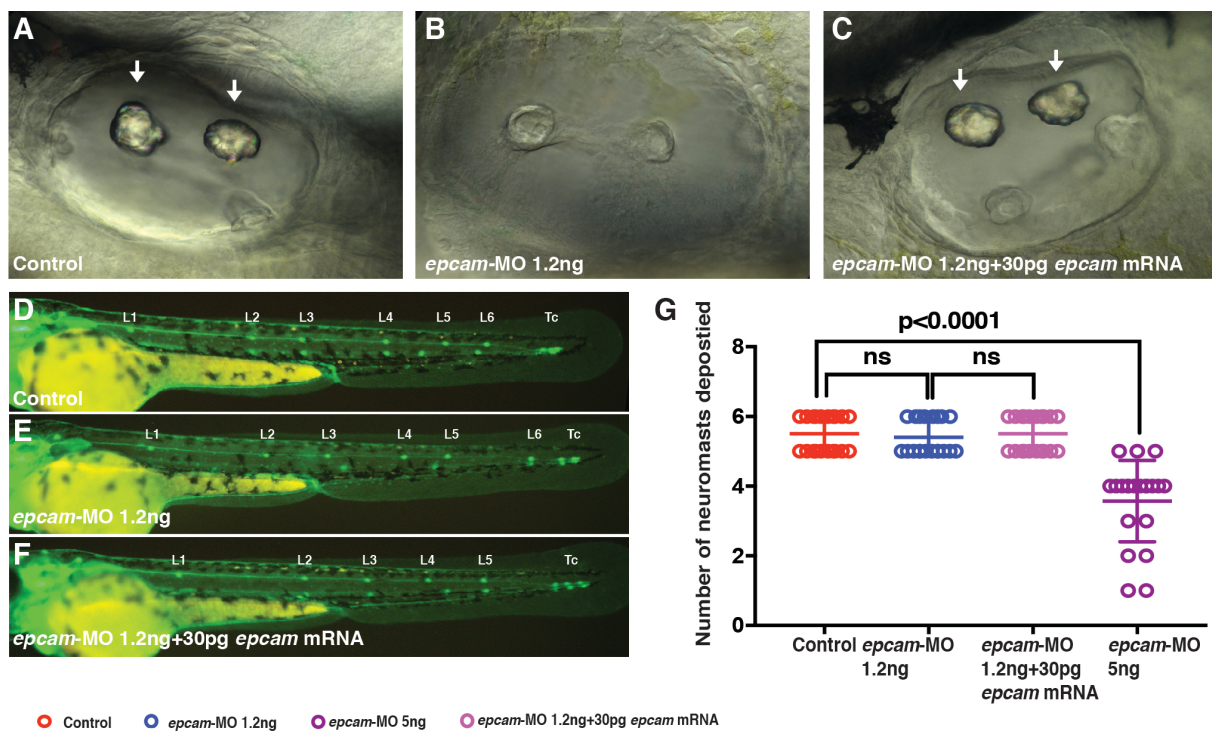


Fig.S5. Validation of *epcam*-MO. (A-C) Injection of 1.2ng *epcam* morpholino recapitulated a previously published *epcam* mutant phenotype. It prevented normal morphogenesis of otoliths (shiny crystals lost- arrows). Co-injection of 30ng rescued this morphant phenotype. (D-G) As in the *epcam* mutants, there was no obvious lateral line phenotype with injection of 1.2ng *epcam*

morpholino. (G) However, when the dose of *epcam* morpholino was increased to 5 ng, a more variable number of neuromasts was deposited, consistent with previous studies that had suggested that the *epcam* morpholinos can have some off-target effects. For our study only the low dose of 1.2 ng was used to minimize potential off target effects.

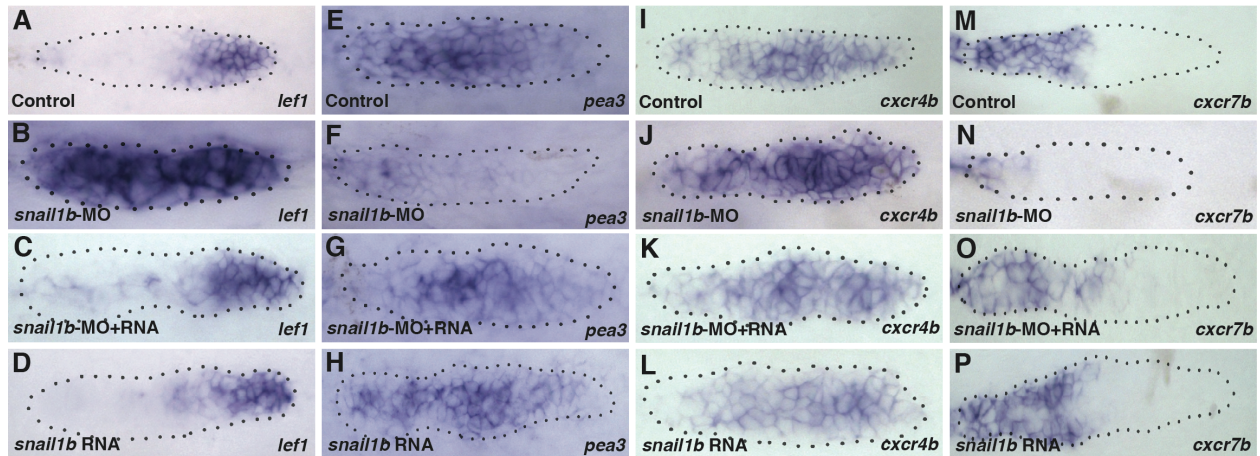
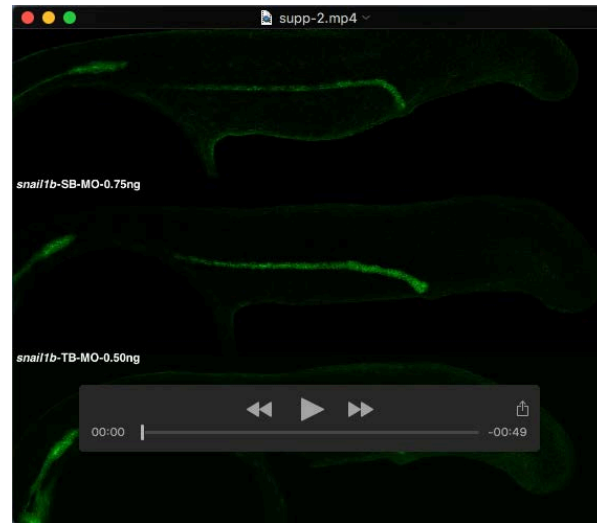
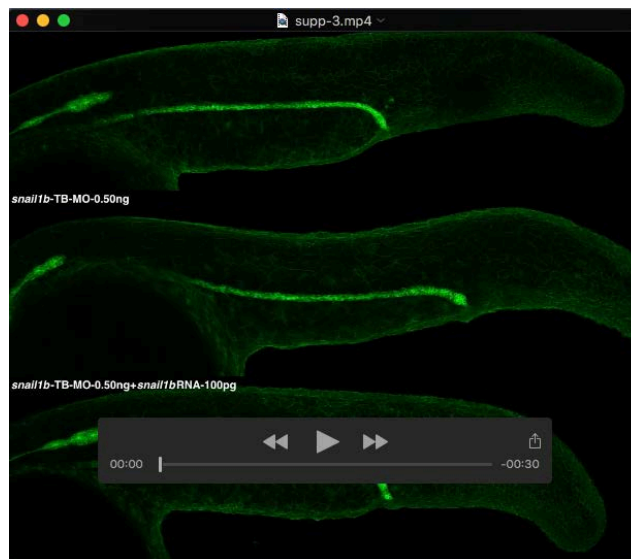


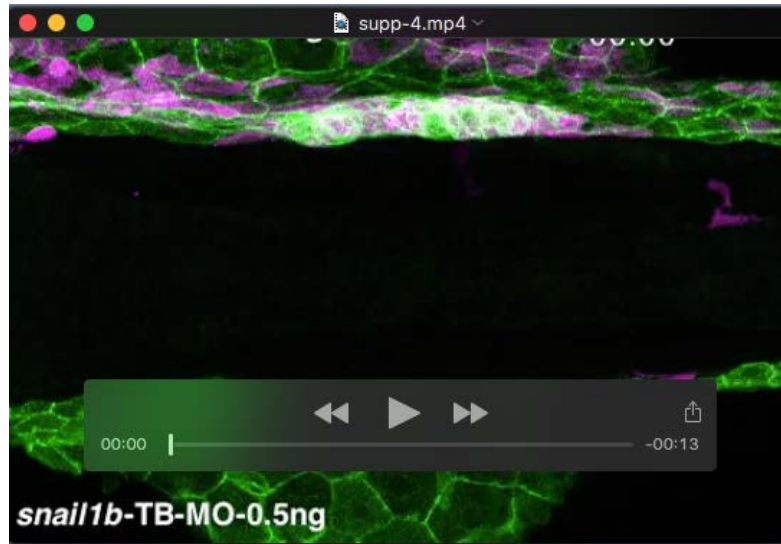
Fig.S6: Rescue of the delayed dynamics of Wnt Fgf signaling systems in *snail1b* morphants by co-injection of *snail1b* mRNA. Expression of *lef1* (A), *pea3* (E), *cxcr4b* (I) and *cxcr7b* (M). *lef1* (B) and *cxcr4b* (J) are expanded into the trailing domain (B), *pea3* (F) and *cxcr7b* (N) are not well established in the trailing domain of *snail1b*-MO. Injection of *snail1b* mRNA along with *snail1b*-TB MO restores the expression patterns of *lef1* (C), *pea3* (G), and *cxcr7b* (O). However, restricted *cxcr4b* expression is not restored (K). Injected of *snail1b* mRNA alone does not have any obvious effect on these signaling systems (D, H, L, P).



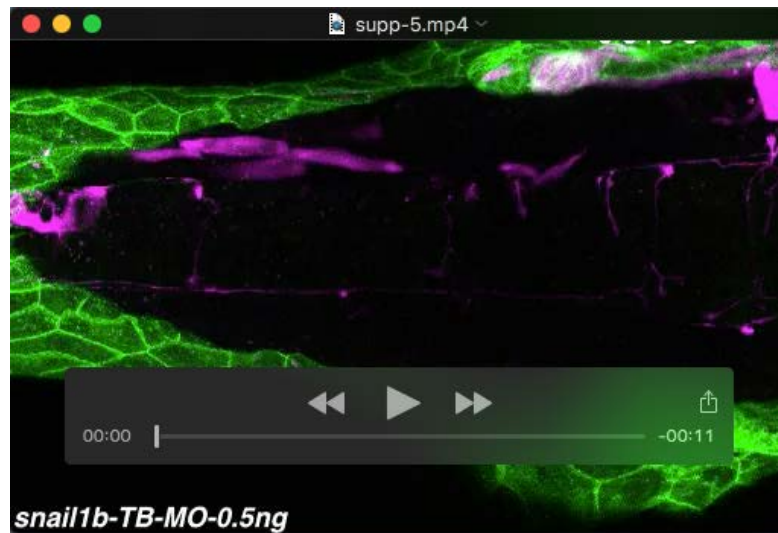
Movie S1. Time-lapse video of pLL primordium migration in control, *snail1b*-TB or SB morphant CldnB:lyn GFP transgenic embryos over approximately 28 hours.



Movie S2. Time-lapse video of pLL primordium migration in control, *snail1b*-TB injected and *snail1b*-TB morpholino and *snail1b* mRNA co-injected CldnB:lyn GFP transgenic embryos. Co-injection of *snail1b* mRNA prevents migratory problems of the primordium in *snail1b*-TB morpholinos injected embryos.



Movie S3. Time-lapse video of a *snail1b*-TB morphant in which non-morphant donor cells (purple) were effectively transplanted into the primordium on the right of the embryo. Migratory behavior is restored in the primordium on the left side which received transplanted non-morphant cells.



Movie S4. Time-lapse video of a *snail1b*-TB morphant shows that migration of the primordium that received transplanted non-morphant cells was not faster when transplanted cells were delivered to the trailing domain of the morphant primordium and not the leading end, where *snail1b* is normally expressed.